

# **ASSESSMENT OF SECONDARY EFFECTS IN POST-TENSIONED FLAT PLATES**

By

AMY HUFNAGEL AND THOMAS H.-K. KANG



Authorized reprint from: December 2012 issue of the PTI Journal

Copyrighted © 2012, Post-Tensioning Institute  
All rights reserved.

# ASSESSMENT OF SECONDARY EFFECTS IN POST-TENSIONED FLAT PLATES

BY AMY HUFNAGEL AND THOMAS H.-K. KANG

*The research was focused on determining the secondary, or hyperstatic, moment of post-tensioned concrete flat plate buildings of different dimensions, as well as investigating the secondary column axial forces induced by post-tensioning. The primary purpose of this research was to develop design charts regarding the secondary moment to aid practicing engineers in the preliminary design of post-tensioned flat plates. Practicing engineers in the post-tensioned building construction industry often struggle to calculate the secondary moment of indeterminate structures because of the interrelation of many different variables, including the degree of post-tensioning and restraints, post-tensioning steel profile, and member sizes. The design aid charts produced contain the secondary moment for these provided building sizes. The other purpose of this research was to investigate the effect of post-tensioning on column axial forces and to determine the possibility of differential column shortening, which may occur at exterior building locations in very tall buildings. This paper describes the methods used in completing the aforementioned charts and analyzes the data and trends found throughout the project.*

## KEYWORDS

Balanced moment; column axial force; flat plates; post-tensioned concrete; primary moment; secondary moment.

## INTRODUCTION

Prestressed concrete encompasses both pre-tensioned and post-tensioned concrete structures, which both use high-strength materials as a means to counteract the stress of gravity loads that are placed on a structure. There are different areas of implementation for pre-tensioned and post-tensioned concrete; however, the focus of this research

is on cast-in-place post-tensioned concrete slabs. Post-tensioning is used for many reasons, including economy and building efficiency as well as the reduction of deflection and cracking it provides. The use of post-tensioning can reduce the depth of slabs and story height, as well as improve the installations of “heating and electrical ducts, plumbing risers, and wall and partition surfaces” (Nilson et al. 2009). Post-tensioned flat plates have already been widely implemented into the design of both residential and commercial structures (Foutch et al. 1990).

This research uses the idea of the application of equivalent or balanced loads as a way to describe the effect of post-tensioning on the structures, that is, the load balancing method (Lin and Burns 1981). The load balancing method can be especially useful for analysis of indeterminate structures such as continuous beams and two-way slabs. In post-tensioned flat plate construction, post-tensioning tendons with variable eccentricity are used to apply such balanced loads throughout the length of the slabs. Different loads can be achieved by different tendon profiles. Free-body diagrams are important tools to visually display the loads applied through post-tensioning, both axially along the tendon and vertically countering the applied loads. With slabs that use tendon eccentricity at the ends, forces at the ends of the beams or slabs may create end moments, although it is not typical for relatively thin two-way slabs.

Many different tendon profiles can be chosen for different building scenarios, and the choice depends on the necessary balanced loads. In buildings with slabs that stretch across multiple columns or supports, the shape of the tendon can be variable along the entire length of the span to best balance the applied loads. If uniformly distributed loads are being applied, the best tendon profile is typically a second-order parabolic shape. It is always important to consider not only the loads involved in the design, but also the economic aspect of the different tendon profiles, quantities of unbonded post-tensioning

---

PTI JOURNAL, V. 8, No. 2, December 2012. Received and reviewed under Institute journal publication policies. Copyright ©2012, Post-Tensioning Institute. All rights reserved, including the making of copies unless permission is obtained from the Post-Tensioning Institute. Pertinent discussion will be published in the next issue of PTI JOURNAL if received within 3 months of the publication.

tendons and bonded reinforcing bars, and slab thickness and span length (Kang and Wallace 2008).

In cast-in-place post-tensioned flat plate construction, the slab is restrained against vertical deformation at the support, and such a restraint causes secondary moments in the slab as well as secondary axial forces in the column, both of which should be considered in the design. However, determination of the induced secondary moments is very cumbersome during the preliminary design stage because of the interrelation of many different variables, including the degree of post-tensioning and restraints, post-tensioning steel profile, and member sizes. The objectives of this research are to determine the secondary moment of post-tensioned concrete flat plates, to provide design aid charts regarding this secondary moment, and to investigate the effect of the forces induced by post-tensioning on the columns as an axial force. The purpose of this paper is to describe the methods used in completing this research, to provide a summary of the data collected, and to analyze the data found throughout the project to draw conclusions about certain characteristics of post-tensioned flat plate design.

## METHODOLOGY

This research was completed in two main portions, the first involving the determination of secondary, or hyperstatic, slab moments ( $M_{sec}$ ) in indeterminate structures; and the second focusing on the secondary effects of post-tensioning on column axial forces. The process for conducting this research involved using a finite element program for both portions of the research.

The secondary moment ( $M_{sec}$ ) is defined as the moment due to reactions induced by prestressing (with a load factor of 1) according to ACI 318-08 (Section 18.10.3) (ACI Committee 318 2008). In monolithic concrete construction, as the columns constrain translation—deflection and rotation of the slab that are caused by post-tensioning—additional reactions are developed in the columns and these additional column axial forces and moments generate hyperstatic (or secondary) moments and shears in the slab (Alaami and Bommer 1999). There are two methods to determine the  $M_{sec}$  value: 1) the direct method; and 2) the indirect method. In the direct method, the column reactions due to post-tensioning can be first obtained by imposing balanced loads on the slabs, and then these column reactions are separately applied to each slab at the top and bottom to determine the secondary moment  $M_{sec}$ . In the indirect method, which was used in this research, first the balanced moment  $M_{bal}$  in the concrete generated

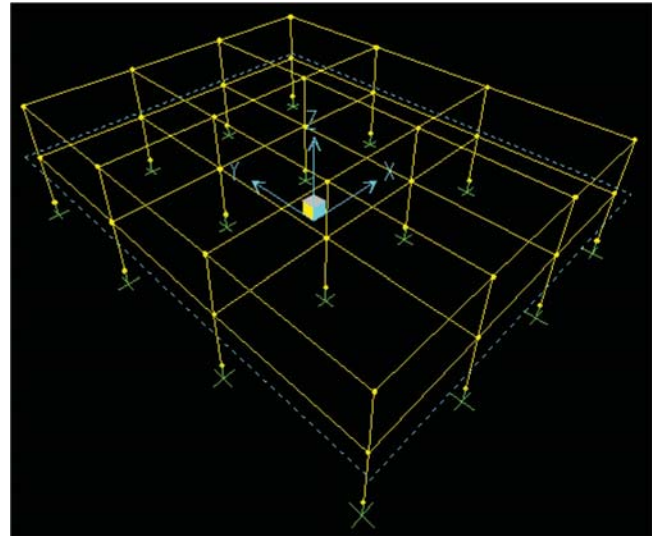


Fig. 1—Office flat plate buildings with 20 x 25 ft slab panels.

by the post-tensioning forces was found for model buildings of different dimensions. Next, the primary moment ( $M_p = eP_e$ ) was found by evaluating the eccentricities  $e$  of the placement of the tendons at certain locations and the effective post-tensioning forces  $P_e$ . Finally, from this information, the secondary moment  $M_{sec}$  was calculated as ( $M_{bal} - M_p$ ). Both the direct and indirect methods would yield the same solution when using the Equivalent Frame Method (refer to ACI 318-08 Sections 13.7 and 18.12.1) (Alaami and Bommer 1999).

For the second portion of the research, the column axial forces induced solely by post-tensioning were found and then analyzed to consider other effects, including differential column shortening. A detailed step-by-step procedure is provided in the following sections.

## Model buildings

A total of 96, 3-bay by 3-bay, two-story model buildings were created in a structural analysis program SAP2000 (CSI 2009) as shown in Fig. 1 and Tables 1 and 2 (refer to Fig. 2 for notation and directions). The selected dimensions of the buildings are typical of those used in actual post-tensioned flat plate construction (PTI Committee DC-20 2010). The dimensions were input to the program, including the story height, bay width, number of bays in each direction, and number of stories. Fixed joint restraints were defined for the bottom of the columns. The concrete used was assumed to have a compressive strength of 5000 psi. For each dimension provided, three trials were used to explore the effect of different column sizes. Keeping all other variables consistent, only the column

**Table 1—Design options for office flat plate building models**

Bay width in transverse direction (x-direction), ft	Slab span length in longitudinal direction (y-direction), ft	Slab thickness, in.
20	25	7.5
	27	8
	30	8.5
25	25	7.5
	27	8
	30	8.5
30	25	8.5
	27	8.5
	30	8.5
35	25	10
	27	10
	30	10

**Table 2—Design options for residential flat plate building models**

Bay width in transverse direction (x-direction), ft	Slab span length in the longitudinal direction (y-direction), ft	Slab thickness, in.
20	21	5.5
	24	6.5
	27	7.5
	30	8
	32	8.5
25	21	7
	24	7
	27	7.5
	30	8
	32	8.5
28	21	7.5
	24	7.5
	27	7.5
	30	8
	32	8.5
30	21	8
	24	8
	27	8
	30	8
	32	8.5

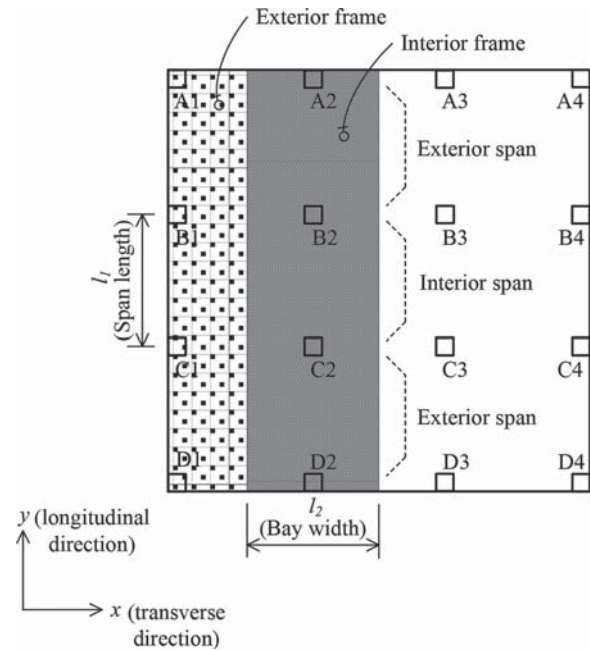


Fig. 2—Model building plan.

sizes were changed from 20 x 20 in. to 24 x 24 in. and 28 x 28 in. The slab-beam sections were defined to function as equivalent slab-beams, using a length  $l_2$  reaching the full transverse span with a thickness  $h$ , as provided, and a width depending on the location of the slab-beam and the tributary area. The interior slab-beams were defined with a width equivalent to the transverse width of the bay, while exterior slab-beams received half of this width plus half of the column transverse width (refer to Fig. 2). The equivalent slab-beams were applied in both directions. The end offsets were defined as half the distance of the column width, embedded halfway into the column, giving the slab-beams a rigid-zone factor of 1. The column stiffness was not reduced, as the stiffness of torsional elements (refer to Section 13.7.2.3 of ACI 318-08) is likely to be significantly higher than that of nonprestressed concrete flat plates due to the in-plane (membrane) constraints provided by the post-tensioning. This was shown from previous experimental studies (Kang 2004; Kang and Wallace 2005) and also is commonly used at both the service limit and ultimate limit states (under gravity loads) in practice (PTI Committee DC-20 2010; also refer to Section 4.3.1 of PTI DC20.9-11 [PTI Committee DC-20 2011]). Figure 1 shows a sample of one of the buildings within the program.

### Factored gravity loads and moments

First, the gravity loads were determined for each building model and applied as trapezoidal loads along the

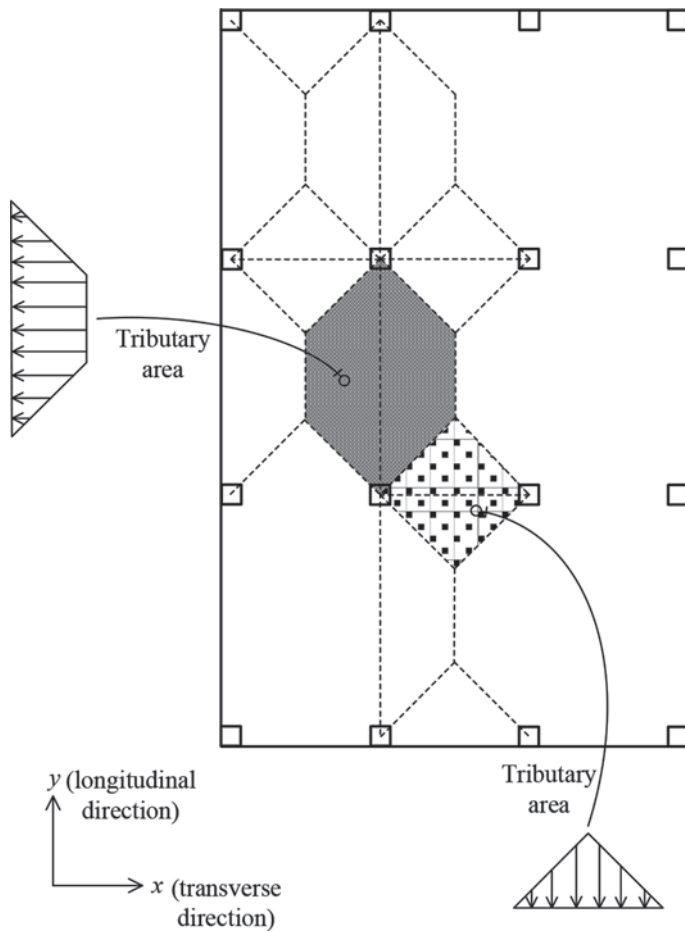


Fig. 3—Gravity load distribution based on tributary area for model buildings with rectangular panels.

length of each slab-beam to account for accurately shaped tributary areas, which can be seen in Fig. 3. For buildings of different bay widths in the two principal directions, the longer bay direction has a trapezoidal gravity load, whereas the load distribution of the shorter bay is triangular (Fig. 3). If the span lengths along both principal directions are equal, the tributary areas are also equal for the slab-beams in each of these directions (Fig. 4).

A dead load was applied based on a unit weight of concrete of 150 lb/ft<sup>3</sup> for both the office and residential buildings. A sustained dead load of 30 lb/ft<sup>2</sup> and a live load of 50 lb/ft<sup>2</sup> were also applied to the office buildings, while a sustained dead load of 10 lb/ft<sup>2</sup> and a live load of 55 lb/ft<sup>2</sup> were applied to the residential buildings. These loads are commonly used in practice (PTI Committee DC-20 2010). Figures 3 and 4 show the loads applied to the building using the load distribution caused by the tributary areas. To determine the factored gravity moments  $M_{u,v}$ , load factors of 1.2 and 1.6 were used for the combined dead

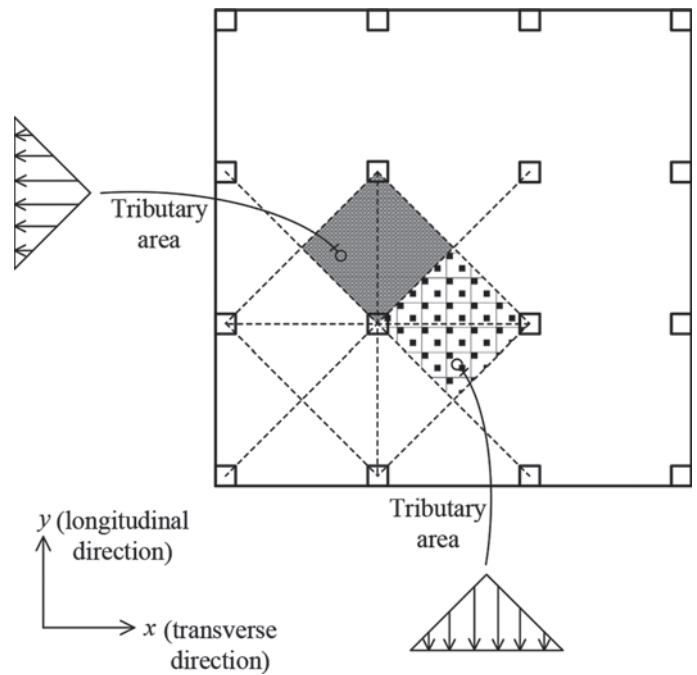


Fig. 4—Gravity load distribution based on tributary area for model buildings with square panels.

loads (sustained dead load in addition to the self-weight of the concrete) and the live loads, respectively, considering only the factored gravity load combination.

### Balanced moments due to post-tensioning

The next step involved finding the balanced moment  $M_{bal}$  due to post-tensioning. For this part, the buildings were again created in SAP2000 (CSI 2009) using the same methods previously discussed. This time, the balanced loads  $\omega_{bal}$  induced by post-tensioning were applied instead of the factored gravity loads. The balanced loads were determined by analyzing the tendon profiles. Parabolic tendon profiles were used, as can be seen in Fig. 5. Also, horizontal end forces due to post-tensioning were applied at the perimeter of each floor (Fig. 5).

The number of tendons was determined to meet ACI 318 flexural and minimum precompression requirements. The tendon starts at the center of gravity of the concrete slab (c.g.c.) at the exterior. Specified clear covers governed the eccentricities of the tendon at the peak of the parabolic shape. The distance from the slab bottom to the lowest point in the parabolic center of gravity of the pressing force (c.g.s.) curve in the exterior span was 1.75 in. (Fig. 5). This point is located in the middle of the exterior span. The highest point of the c.g.s. curve can be

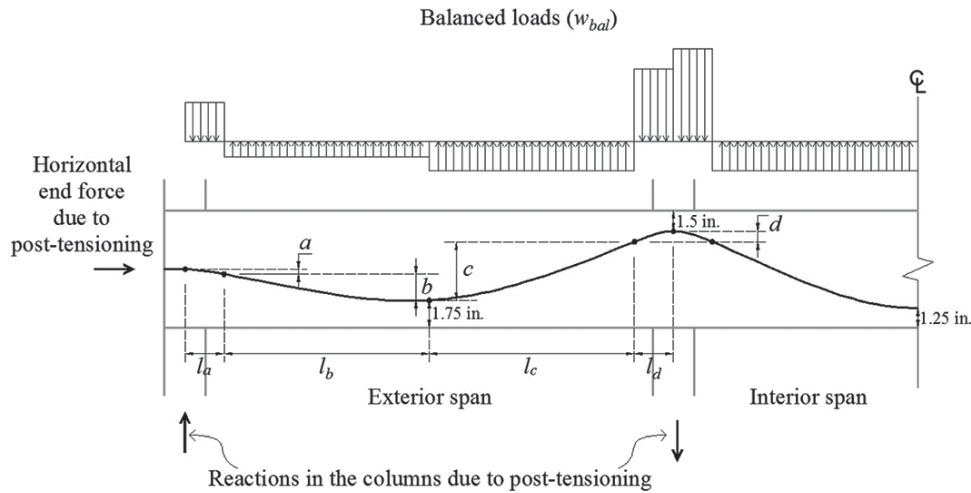


Fig. 5—Tendon profile and balanced loads induced by post-tensioning.

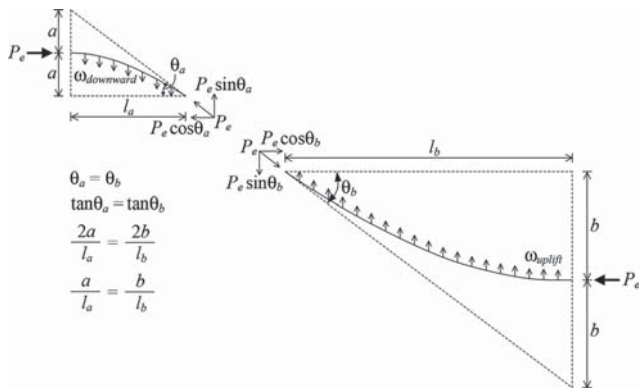


Fig. 6—Free body diagram of tendon at exterior half of exterior span.

found over the interior column centerline, 1.5 in. from the top of the slab. The distance from the soffit to the lowest c.g.s. for the interior span is 1.25 in. The tendon c.g.s. values used are based on typical practice (PTI Committee DC-20 2010) and consistent with those in Chapter 6 of PTI DC20.9-11.

Another important aspect of parabolic tendon profiles is the presence of inflection points along the length of the tendon. In this profile, two can be found in each span. These changes in curvature create both upward and downward forces due to post-tensioning. The change in direction of the force at the inflection points of the tendon is illustrated in Fig. 5. To provide a smooth transition between the changes in positive and negative curvature, the inflection points must be located at specific locations that satisfy the following conditions (refer to Fig. 6 for derivation and notation).

$$\frac{a}{l_a} = \frac{b}{l_b} \quad (1)$$

$$\frac{c}{l_c} = \frac{d}{l_d} \quad (2)$$

where  $a$ ,  $b$ ,  $c$ , and  $d$  are the vertical distances between the c.g.s. and the inflection point as shown in Fig. 5, and  $l_a$ ,  $l_b$ ,  $l_c$ , and  $l_d$  are the lengths of portions of the span considered as shown in Fig. 5. These conditions were based on the basic geometry of the tangential force at the location of the inflection points. The heights and lengths shown in Fig. 5 are dependent on one another in the determination of the inflection points. The geometrical conditions ensured that the length of the slab span and the thickness of the slab were both considered accurately, as well as ensured that the angles shown in Fig. 6 were equal. Although many different scenarios related length between inflection points and distance between inflection point and maximum and minimum heights of the tendon in a way that satisfied the tangential force equilibrium, typical tendon profiles influenced the final choice of inflection point location. In this study, the inflection points were located at 8 and 92% of the length of the span ( $\sim l_2/12$ ), with the lowest point of the tendon at the exact center of the span, for both the interior and exterior spans.

The balanced loads applied through post-tensioning involved upward and downward uniformly distributed

forces of differing magnitudes due to the presence of these inflection points. An example of the loads induced by post-tensioning can be seen in Fig. 5. The placement of the inflection points at these specific positions resulted in a smooth transition between positive and negative curvature as well as an equilibrium of vertical balanced loads acting on the concrete slab within a given floor. The uniform downward load applied by each tendon at the left-hand edge of the exterior span (refer to Fig. 5 or 6) was found using Eq. (3), while the uniform upward load was found using Eq. (4).

$$\omega_{\text{downward}} = P_e \sin \theta_a \approx P_e \tan \theta_a = P_e \left( \frac{2a}{l_a} \right) \quad (3)$$

$$\omega_{\text{uplift}} = P_e \sin \theta_b \approx P_e \tan \theta_b = P_e \left( \frac{2b}{l_b} \right) \quad (4)$$

where  $P_e$  is the total effective stress of tendons, and  $\theta_a$  and  $\theta_b$  are the angle between the horizontal line and tangential line at the inflection point, respectively, as shown in Fig. 6.

The buildings were all analyzed to view the deflected shape as well as the shear and moment diagrams. The moments produced ( $M_{\text{bal}}$ ) have the opposite effect of the factored gravity moments  $M_u$ ; therefore, the locations of negative and positive moments are opposite (Fig. 7).

### Primary moment

The primary moment  $M_p$  was hand-calculated by taking into account the force applied by the amount of steel used in each tendon, the number of tendons used, and the eccentricity of each tendon as follows

$$M_p = P_e e \quad (5)$$

where  $e$  is the tendon eccentricity with respect to the c.g.c (that is, the distance between the c.g.s. and c.g.c.). The number of tendons needed for each span was first determined based on the minimum precompressive stress  $f_{pc}$  in the concrete due to the tendons—125 psi as specified by ACI 318-08 Section 18.12.4. Note that the effective force applied for each Grade 270, 1/2 in. diameter tendon (cross-sectional area  $A_{ps} = 0.153 \text{ in.}^2$ ) is approximately 27 kips, 65% of the ultimate tensile force of a tendon

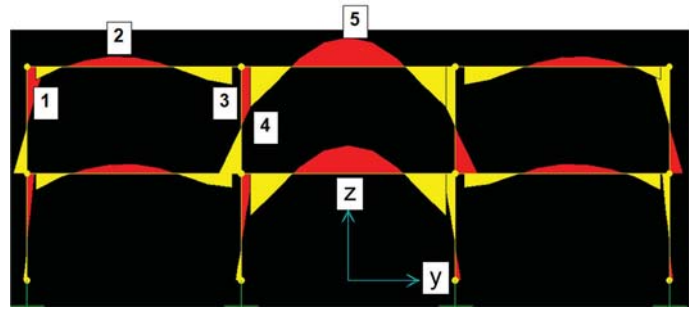


Fig. 7—Balanced moment diagram of exterior frame for office building model with 20 x 25 ft slab panels and 20 x 20 in. columns.

( $A_{ps} f_{pu}$ ). The number of tendons was then confirmed or modified based on the nominal moment strength check, as will be discussed later in this paper. Table 3 presents the number of tendons used for each model.

### Secondary moment

The secondary, or hyperstatic, moment  $M_{\text{sec}}$  is generated from column reactions induced by post-tensioning. After finding the primary moment and the balanced moment due to post-tensioning, the secondary moment was found using the following equation (that is, the indirect method).

$$M_{\text{sec}} = M_{\text{bal}} - M_p \quad (6)$$

Note that no load factors are taken into account in Eq. (6). Table 4 shows the secondary moments at five locations for the selected office building model (all 96 model results are available in Appendix A\* or by Hufnagel [2011]). Because the dimensions of the building are symmetric, only half of the moments across the length of the building were considered (Fig. 7). Only the y-direction of the building was considered (refer to Fig. 2 for the y-direction) because this was the variable in question for each scenario. Additionally, Table 4 provides the values for the factored gravity moments, moments used to compute required strength ( $M_{\text{req'd}} = \phi M_u + M_{\text{sec}}$ ), and design moment strengths ( $\phi M_n$ ) for the selected locations. The design moment strength is discussed in the following section.

\*This Appendix includes the design charts mentioned in this paper; it can be downloaded from the PTI website at [www.post-tensioning.org](http://www.post-tensioning.org).

**Table 3—Total number of tendons designed for building models**

Building type	Bay width or span length, ft		Total number of tendons			
			Longitudinal (y-direction)		Transverse (x-direction)	
	Transverse	Longitudinal	Exterior	Interior	Exterior	Interior
Office	20	25	5	9	6	11
		27	5	9	7	13
		30	5	10	8	15
	25	25	6	11	6	11
		27	6	12	7	13
		30	6	12	8	15
	30	25	8	15	6	12
		27	8	15	7	13
		30	8	15	8	15
	35	25	10	20	7	14
		27	10	20	8	16
		30	10	20	9	17
Residential	20	21	4	7	4	7
		24	4	8	5	9
		27	5	9	6	12
		30	5	9	7	14
		32	5	10	8	16
	25	21	5	10	5	9
		24	5	10	5	10
		27	6	11	6	12
		30	6	11	7	14
		32	6	11	8	16
	28	21	6	12	5	9
		24	6	12	6	11
		27	6	12	6	12
		30	7	13	7	14
		32	7	14	8	16
	30	21	7	14	5	10
		24	7	14	6	11
		27	7	14	7	13
		30	7	14	7	14
		32	8	15	8	16

### Design moment strength

First, the required amount of bonded reinforcing bars was determined. The bonded steel reinforcement used in the slabs was determined as per ACI 318-08 Section 18.9. Number 4 and 5 bars were considered, as these are typical sizes for post-tensioned concrete slabs. Next, the following equation was used to determine the design moment strength at the five selected locations.

$$\phi M_n = A_p f_{ps} \left( d_p - \frac{a}{2} \right) + A_s f_y \left( d - \frac{a}{2} \right) \quad (7)$$

where  $\phi$  is the strength reduction factor (= 0.9 for this project);  $A_p$  is the total area of post-tensioning tendons;  $f_{ps}$  is the tendon stress at nominal moment strength;  $d_p$  is the distance from the extreme compression fiber to the centroid of post-tensioning tendons;  $a$  is the depth of the rectangular stress block;  $A_s$  is the total area of bonded reinforcement;  $f_y$  is the yield strength of bonded reinforcement; and  $d$  is the distance from the extreme compression fiber to the centroid of bonded tension reinforcement. The design moment strength was then compared to the required moment strength to ensure that it satisfied the strength requirement according to Section 18.10.3 of the

**Table 4—Data at five locations of exterior frame for office building model with 20 x 25 ft slab panels and 20 x 20 in. columns**

Location*	$M_{bal}$ , in.-kip		$M_p$ , in.-kip		$M_{sec}$ , in.-kip		$M_u$ , in.-kip		$M_{req'd}$ , in.-kip		$\phi M_n$ , in.-kip	
	First floor	Roof	First floor	Roof	First floor	Roof	First floor	Roof	First floor	Roof	First floor	Roof
1	218.7	197.7	0	0	218.7	197.7	-913.3	-831.8	-694.6	-634.1	-1657.1	-1657.1
2	-145.5	-148.5	-268.5	-268.5	123	120.1	565.3	588.8	688.3	708.8	2255.7	2255.7
3	305.8	320.9	302.1	302.1	3.7	18.8	-984.2	-1018.8	-980.5	-1000	-2330.6	-2330.6
4	398.3	395.7	302.1	302.1	96.2	93.6	-960.8	-965.3	-864.6	-871.7	-2330.6	-2330.6
5	-221.7	-224.4	-335.6	-335.6	113.9	111.3	553.4	548.8	667.2	660	2405.4	2405.4

\*Location 1: exterior end of exterior span (refer to Fig. 7); Location 2: middle of exterior span (refer to Fig. 7); Location 3: interior end of exterior span (refer to Fig. 7); Location 4: interior end of interior span (refer to Fig. 7); and Location 5: middle of interior span (refer to Fig. 7).

Notes: Positive moment: moment that causes tensile strain at the bottom of the slab; negative moment: moment that causes tensile strain at the top of the slab.

ACI 318-08 requirements, which is as follows

$$\phi M_n \geq M_u + M_{sec} \quad (8)$$

Some of the model buildings needed extra bonded mild steel or add-tendons for the interior frames. The majority of the insufficiencies were found in the interior frames of the buildings in the locations near the columns. Adding more reinforcing bars may be the more cost-effective solution for those with minor deficiencies; however, for some buildings, it may be more logical to use add-tendons rather than a large number of extra reinforcing bars at each location.

### Secondary column axial forces

This procedure was performed using many of the same method described in the preceding sections. First, several building scenarios were created within SAP2000 (CSI 2009), all of which had slab thicknesses of 8 in., floor heights of 10 ft, and column dimensions of 20 x 20 in. Varying span lengths were used, as can be seen in Table 5. Next, equivalent forces induced by post-tensioning were only applied as balanced loads ( $\omega_{bal}$ ) using the same methods as discussed previously in this paper (no gravity loads). The buildings were then analyzed within the program to determine axial forces for both the upper and lower columns in the building. To interpret the data in general terms, the numbers were first normalized by the concrete axial capacity, which takes into account the cross-sectional area  $A_g$  of the concrete column, as well as the compressive strength ( $f'_c = 5$  ksi) of the concrete.

### ANALYSIS

The data collected from the first portion of this research procedure, or the design aid charts, can be found

**Table 5—Information of building models used for assessment of column axial forces**

Case	Stories	Bays per direction	Story height, ft	Span x, ft	Span y, ft
1	2	3	10	20	21
2	2	3	10	20	27
3	2	3	10	25	27
4	2	3	10	20	30
5	2	3	10	25	30
6	2	3	10	28	30
7	2	3	10	30	21
8	2	3	10	30	24
9	2	3	10	30	27
10	2	3	10	30	30

in Appendix A. These tables contain the calculated design moment strength  $\phi M_n$ , the required moment  $M_{req'd}$ , the factored gravity moment  $M_u$ , and the secondary moment  $M_{sec}$  for both interior and exterior frames, as well as the variations in column size. All moments are given in units of kip-in. Table 4 only shows data for an office building with the column measuring 20 x 20 in., although data were accumulated for both the office and residential buildings, for both the interior and exterior frames, and for column widths of 20, 24, and 28 in., as documented in Appendix A. The design aid charts included in Appendix A can be useful for practicing engineers during the preliminary design of buildings of similar dimensions and loads. These charts can be used for a quick check in the determination of secondary moment, which can be difficult to calculate manually.

Data collected throughout the second part of the research can be found in Table 6, which shows the

**Table 6—Column axial forces only due to post-tensioning**

Case	Floor	A1	A2	A3	B1	B2	B3	C1	C2	C3	D1	D2	D3
1	1	-3.67	-0.94	-0.95	-0.93	5.52	5.49	-0.91	5.55	5.52	-3.66	-0.91	-0.93
	2	-1.64	-0.33	-0.34	-0.33	2.30	2.28	-0.32	2.31	2.30	-1.63	-0.32	-0.33
2	1	-3.44	-1.36	-1.37	0.01	4.75	4.73	0.03	4.79	4.77	-3.42	-1.33	-1.34
	2	-1.47	-0.37	-0.37	-0.01	1.82	1.82	-0.02	1.85	1.84	-1.46	-0.35	-0.36
3	1	-3.42	-1.13	-1.14	-0.65	5.18	5.15	-0.63	5.21	5.18	-3.41	-1.11	-1.12
	2	-1.49	-0.37	-0.38	-0.22	2.07	2.06	-0.21	2.09	2.07	-1.48	-0.36	-0.37
4	1	-3.25	-1.45	-1.46	0.02	4.63	4.61	0.05	4.67	4.66	-3.24	-1.41	-1.42
	2	-1.38	-0.37	-0.37	-0.03	1.76	1.76	-0.02	1.78	1.78	-1.37	-0.35	-0.36
5	1	-2.93	-1.14	-1.16	-0.36	4.41	4.39	-0.35	4.44	4.42	-2.92	-1.12	-1.13
	2	-1.27	-0.36	-0.37	-0.14	1.75	1.74	-0.13	1.77	1.76	-1.27	-0.35	-0.35
6	1	-3.71	-1.41	-1.42	-1.04	6.15	6.12	-1.03	6.18	6.15	-3.70	-1.38	-1.40
	2	-1.68	-0.54	-0.54	-0.41	2.62	2.60	-0.41	2.63	2.62	-1.67	-0.52	-0.53
7	1	-3.20	-0.19	-0.21	-1.47	4.87	4.83	-1.46	4.89	4.85	-3.19	-0.17	-0.19
	2	-1.36	-0.11	-0.12	-0.40	1.89	1.87	-0.40	1.90	1.88	-1.36	-0.10	-0.11
8	1	-3.32	-0.44	-0.44	-1.26	5.11	4.96	-1.27	5.05	4.92	-3.29	-0.50	-0.39
	2	-1.44	-0.18	-0.18	-0.37	2.05	1.97	-0.38	2.01	1.95	-1.43	-0.21	-0.16
9	1	-3.40	-0.80	-0.82	-1.01	5.21	5.17	-1.00	5.23	5.20	-3.38	-0.78	-0.80
	2	-1.48	-0.30	-0.30	-0.32	2.09	2.08	-0.31	2.11	2.09	-1.48	-0.29	-0.29
10	1	-3.25	-0.98	-0.99	-0.98	5.19	5.16	-0.96	5.22	5.19	-3.24	-0.96	-0.97
	2	-1.42	-0.34	-0.35	-0.34	2.10	2.09	-0.34	2.12	2.10	-1.41	-0.33	-0.34

All units: kips.

**Table 7—Ratio of column axial forces ( $P_1/P_2$ ) between first and second floors only due to post-tensioning**

Case	A1	A2	A3	B1	B2	B3	C1	C2	C3	D1	D2	D3
1	2.24	2.85	2.79	2.82	2.4	2.41	2.84	2.4	2.4	2.25	2.84	2.82
2	2.34	3.68	3.7	-1*	2.61	2.6	-15*	2.59	2.59	2.34	3.8	3.72
3	2.3	3.05	3	2.95	2.5	2.5	3	2.49	2.5	2.3	3.08	3.03
4	2.36	3.92	3.95	-0.7*	2.63	-2.6*	-2.5*	2.62	2.62	2.36	4.03	3.94
5	2.31	3.17	3.14	2.57	2.52	2.52	2.69	2.51	2.51	2.3	3.2	3.23
6	2.21	2.61	2.63	2.54	2.35	2.35	2.51	2.35	2.35	2.22	2.65	2.64
7	2.35	1.7	1.75	3.68	2.58	2.58	3.65	2.57	2.58	2.35	1.7	1.73
8	2.31	2.44	2.44	3.41	2.49	2.52	3.34	2.51	2.52	2.3	2.38	2.44
9	2.3	2.67	2.73	3.16	2.49	2.49	3.23	2.48	2.49	2.28	2.69	2.76
10	2.29	2.88	2.83	2.88	2.47	2.47	2.82	2.46	2.47	2.3	2.91	2.85

\*The axial force is close to zero either in compression or in tension.

percentage of the column axial force to the concrete axial capacity for each of story of each building. Negative numbers designate columns in tension, while positive number correlate to compression. They are organized by column number designation, which is illustrated in Fig. 2, as well as their building case number, which can be found in Table 5.

Table 7 shows the ratio of axial forces ( $P_1/P_2$ ) between the first and second floors as determined by the numbers found in the structural analysis program (CSI 2009), where  $P_1$  and  $P_2$  are the column axial forces due to post-tensioning in the first- and second-floor columns, respectively. Most of the ratios exceed 2 significantly, and the ratio is as high as 4

**Table 8—Differential column shortening**

Case	Floor	Differential column force, kips				Differential column shortening, in.			
		A1-A2	B1-B2	C1-C2	D1-D2	A1-A2	B1-B2	C1-C2	D1-D2
1	First	-2.73	-6.45	-6.46	-2.75	-0.00030	-0.00068	-0.00068	-0.00030
	Roof	-1.31	-2.63	-2.63	-1.31	—	—	—	—
2	First	-2.08	-4.74	-4.76	-2.09	-0.00024	-0.00049	-0.00049	-0.00024
	Roof	-1.1	-1.83	-1.852	-1.11	—	—	—	—
3	First	-2.29	-5.83	-5.84	-2.3	-0.00025	-0.00060	-0.00061	-0.00025
	Roof	-1.12	-2.29	-2.3	-1.12	—	—	—	—
4	First	-1.8	-4.61	-4.62	-1.83	-0.00021	-0.00048	-0.00048	-0.00021
	Roof	-1.01	-1.79	-1.8	-1.02	—	—	—	—
5	First	-1.79	-4.77	-4.79	-1.8	-0.00020	-0.00050	-0.00050	-0.00020
	Roof	-0.91	-1.89	-1.9	-0.92	—	—	—	—
6	First	-2.3	-7.19	-7.21	-2.32	-0.00026	-0.00076	-0.00076	-0.00026
	Roof	-1.14	-3.03	-3.04	-1.15	—	—	—	—
7	First	-3.01	-6.34	-6.35	-3.02	-0.00032	-0.00064	-0.00064	-0.00032
	Roof	-1.25	-2.29	-2.3	-1.26	—	—	—	—
8	First	-2.88	-6.37	-6.32	-2.79	-0.00031	-0.00065	-0.00065	-0.00030
	Roof	-1.26	-2.42	-2.39	-1.22	—	—	—	—
9	First	-2.6	-6.22	-6.23	-2.6	-0.00028	-0.00064	-0.00064	-0.00028
	Roof	-1.18	-2.41	-2.42	-1.19	—	—	—	—
10	First	-2.27	-6.17	-6.18	-2.28	-0.00025	-0.00064	-0.00064	-0.00025
	Roof	-1.08	-2.44	-2.46	-1.08	—	—	—	—

at the column location D2 of the Case 4 building (refer to Table 7 and Fig. 2). This implies that the reactions due to post-tensioning of the roof floor are smaller than those of the first floor. Otherwise, the axial force ratio between the first and second floors would have been approximately 2.

Because some of the columns were found to be in compression and some in tension, this also poses a potential problem of differential column shortening ( $\delta_{diff}$ ) between the exterior and interior columns. To quantify these effects, the column shortening  $\delta$  was found for each column based on the following equation.

$$\delta = \frac{\Delta PL_{col}}{A_g E_c} \quad (9)$$

where  $\delta$  is the column axial deformation;  $\Delta P$  is the column axial force only due to post-tensioning;  $L_{col}$  is the column height;  $A_g$  is the gross cross-sectional column area; and  $E_c$  is the modulus of elasticity of concrete, estimated to be  $57,000\sqrt{f'_c}$ . This equation was used for all columns, including

those on the first and second floors. It was confirmed that the sum of the column axial forces in all columns at each floor was equal to zero. The differential column shortening  $\delta_{diff}$  was obtained from the difference ( $\delta_{int} - \delta_{ext}$ ) in column axial deformation between adjacent interior and exterior columns. Maximum differential column shortening was observed between a corner column and an adjacent interior column. The two floors were then combined to give the total differential column shortening at the base level, which is shown in Table 8.

## DISCUSSION OF RESULTS

### Secondary slab moments

Figures 8 through 11 show the moment diagrams for the different moments found in the first portion of the research for the office building with 20 x 25 ft slab panels and 20 x 20 in. columns. These diagrams show the opposite effects of the factored gravity loads and the balanced loads and are also useful in analyzing the relationship between the different variables. The balanced moment diagram has

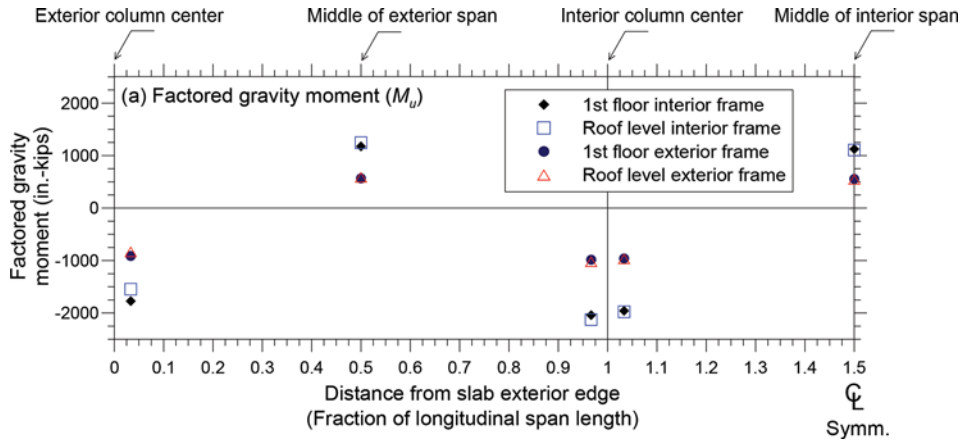


Fig. 8—Factored gravity moment diagram for office building model with 20 x 25 ft slab panels and 20 x 20 in. columns.

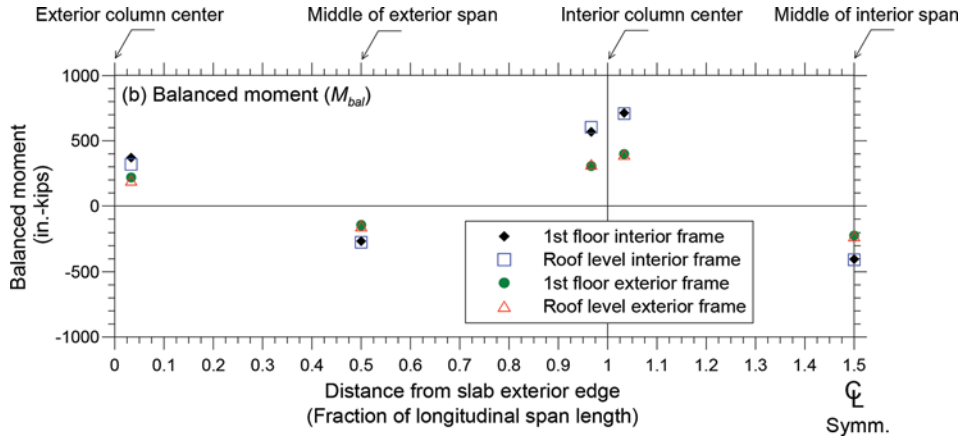


Fig. 9—Balanced moment diagram for office building model with 20 x 25 ft slab panels and 20 x 20 in. columns.

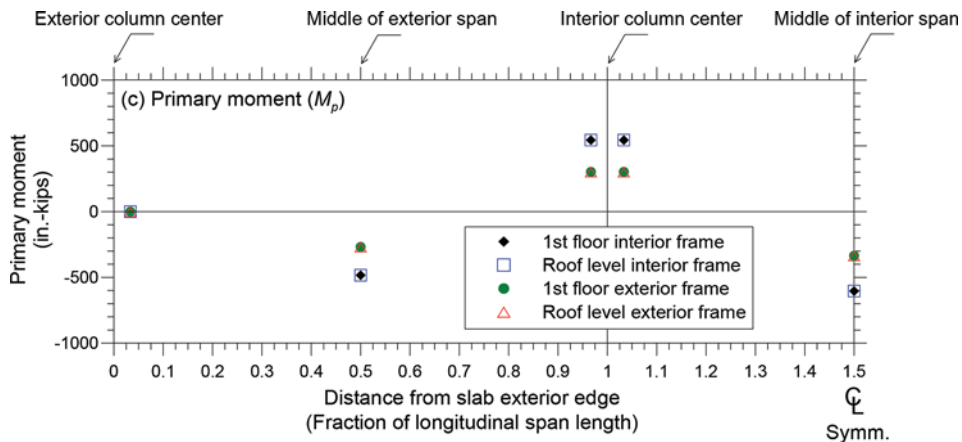


Fig. 10—Primary moment diagram for office building model with 20 x 25 ft slab panels and 20 x 20 in. columns.

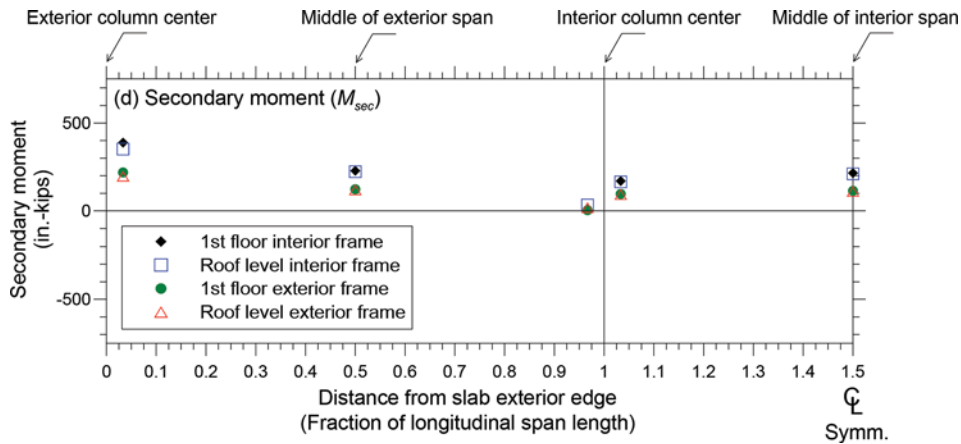


Fig. 11—Secondary moment diagram for office building model with 20 x 25 ft slab panels and 20 x 20 in. columns.

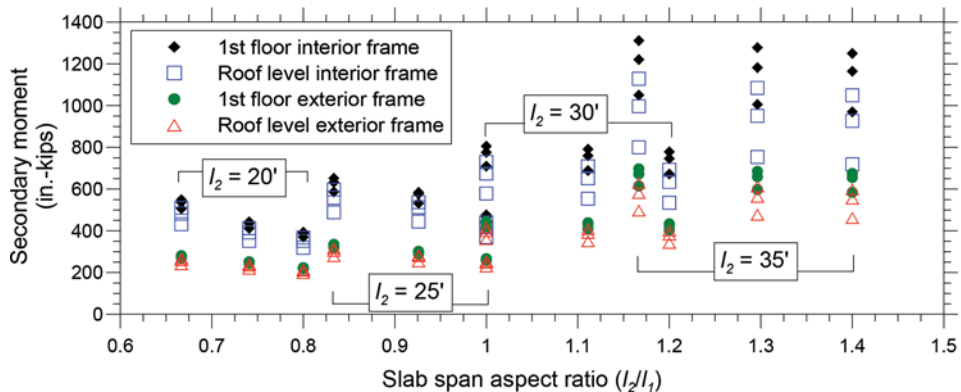


Fig. 12—Secondary moment versus slab span aspect ratio ( $l_2/l_1$ ) for various longitudinal span lengths ( $l_2$ ).

a parabolic shape, as does the primary moment diagram. When the primary moment is subtracted from the balanced moment, the result is the secondary moment, which exhibits an essentially linear shape (Fig. 11).

Notable trends were found in analyzing the data collected in the design tables. The dimensions of the buildings seem to directly correlate to the magnitude of the secondary moment. For each building dimension ( $l_2$ ) provided for the transverse direction, several options were given for the longitudinal direction (refer to Fig. 12). As the length of  $l_2$  increases, the value found for the secondary moment increases in magnitude. Also, for the given  $l_2$ , the span aspect ratio of  $l_2$  to  $l_1$  affects the magnitude of the secondary moment  $M_{sec}$  (Fig. 12); the larger the longitudinal span length  $l_2$ , the greater  $M_{sec}$  will be (all other parameters being equal). These trends are mainly due to the fact that the more tendons are used for the larger  $l_2$ , as indicated in Table 3. The information on the magnitude of  $M_{sec}$  may be

useful to practicing engineers, who may be able to formulate better estimates after looking at the trends in the data and comparing to the dimensions and loads of the building being designed.

For interior frames, the secondary moments are typically much higher in magnitude. This can be partially attributed to the fact that more post-tensioning tendons are used in the tributary area of the interior frames than that of the exterior frames. For both interior and exterior frames, the secondary moments increased with the increased column dimension in the longitudinal direction, except adjacent to the interior columns where an increase in column dimension seems to decrease the secondary moment slightly. These trends were found in the data for both the office buildings and the residential buildings (refer to Appendix A).

As expected, the loads applied on the buildings with the larger longitudinal spans created factored gravity moments ( $M_u$ ) of greater magnitudes. The increase in these moments,

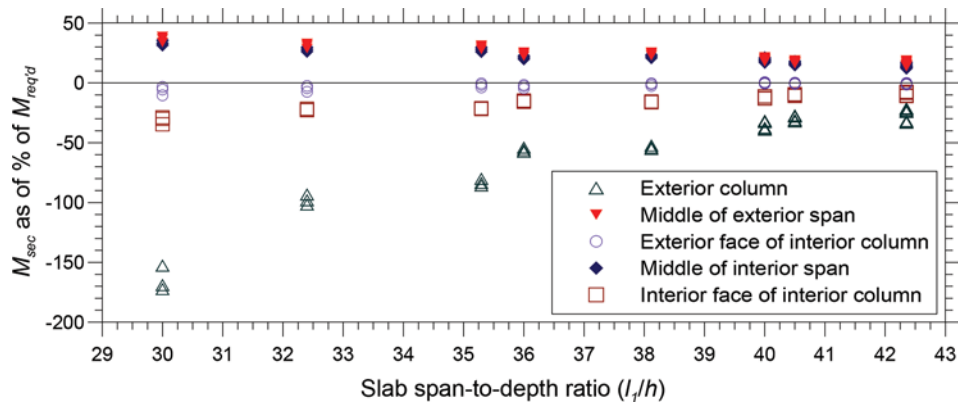


Fig. 13—Secondary moment as of percentage of required moment versus slab span-depth ratio ( $l_1/h$ ).

combined with the increase in secondary moments, results in a greater required moment at the midspan, where the maximum positive gravity moment occurs. At the end of each span, on the other hand, the increase in (positive) secondary moment results in a smaller required moment, as it has the opposite sign of the (negative) factored gravity moment. However, when the post-tensioned flat plate frame is subjected to significant lateral loading, causing a positive moment at the face of the column, the positive secondary moment can be a critical issue in the slab design. This is particularly true at the exterior connection and at the interior face of the interior column. The amount of the secondary moment at the exterior face of the interior column is typically very small or almost negligible (Fig. 11). Figure 10 also compares secondary moments in the first-floor and roof levels, indicating the fact that the lower floor slabs experienced greater numbers in comparison to the upper-floor slabs.

Figure 13 shows a graph comparing the percentage of the secondary moment with regard to the factored gravity moment against the slab span-depth ratio. The secondary moment can be as much as 40% of the required positive moment for some of the buildings; however, this number decreases as the slab span-depth ratio increases. This means that although large span buildings typically have larger secondary moments in comparison to smaller span buildings, the secondary moment may affect the smaller buildings more drastically as it is a much larger portion of the required moment. At the corner connections of smaller buildings, the secondary moment is even greater than the factored negative gravity moment (Fig. 11); thus, the gravity load combination generates the positive required moment demand at the corner of those buildings.

## Comparison to results from ADAPT-Builder Floor Pro

Results of the model buildings from the research completed using SAP2000 were compared to those done using ADAPT-Builder Floor Pro 2010 (ADAPT 2010), a three-dimensional finite element program commonly used in the industry. It is noted that ADAPT-Builder employs only the finite element method (not the Equivalent Frame Method incorporated in ADAPT-PT). This program models each floor individually and is not capable of modeling a multi-story system.

First, a floor slab of the selected building was modeled (Fig. 14). Ten-foot columns with fixed end restraints were provided on the bottom of the slab; however, the presence of the top column really did not affect the ADAPT-Builder results of the secondary moment, nor did the column end boundary (or restraint) conditions. The same number of tendons used previously remained consistent. Banded tendons in the N-S direction and distributed tendons in the E-W direction were used. The same parabolic tendon profile was attempted to be used as previously discussed. Note that the lowest and highest points of the c.g.s. curve as well as inflection point locations can only be input in the ADAPT-Builder.

For each design section, secondary moment diagrams can be viewed, and these secondary moments of the interior and exterior frames for the selected model buildings are indicated in Table 9. A comparison of the values for secondary moments acquired from SAP2000 and ADAPT-Builder can also be found in Table 9. In analyzing the data, the values for secondary moments from the two programs vary a significant amount; however, the trends are very similar. Both produced essentially linear distributions of hyperstatic moment within a span for each frame (Fig. 15 and 16), with the peak value nearest to the exterior column

of the exterior spans of each frame, or Location 1, as previously specified. The locations of interest in the interior span of each frame showed very similar values, while the lowest recorded secondary moment was found near the interior column in the exterior span of each frame.

The difference in values acquired between the two programs seems most significant at the location near the interior column in the exterior span of each frame. While this location was consistently the area of smallest secondary moment, SAP2000 recorded somewhat lower values than that of ADAPT-Builder. On the other hand, at the location near the exterior column in the exterior span, the secondary moment monitored from ADAPT-Builder was consistently lower than that of SAP2000. Possible reasons for discrepancies between the values between the two problems include many differences in modeling. SAP2000 modeled two-story buildings with three bays, or four frames, in each direction. ADAPT-Builder was capable of modeling only one story in each simulation, not reflecting the discrepancy in the boundary conditions at the bottom of the column. Given the fact that the column end fixity and the presence of the top column did not affect the secondary moment results, the boundary restraints used for the column bottom supports in ADAPT-Builder appear to be simple supports, which may lead to a more flexible system than that in SAP2000. On the other hand, the Equivalent Frame Method used in this study did not account for the reduced column stiffness due to the torsional element's flexibility, as the in-plane constraints provided by the post-tensioning were considered significant. The rigid torsional stiffness, however, might have slightly overestimated the stiffness of a flat plate frame.

Another possible reason for finding different results in ADAPT-Builder is that the ADAPT-Builder analysis uses the direct method to determine the secondary moment in three-dimensional (3-D) finite element models whereas SAP2000 uses the indirect method in connection with the Equivalent Frame Method. It is also worth mentioning that the presented results in ADAPT-Builder are not exactly symmetric with respect to the centerline (midspan) of the interior span (Fig. 15 and 16), possibly due to the asymmetric mesh used for the simulation (they were meshed automatically in ADAPT-Builder). Overall, the produced secondary moment diagrams are useful in a comparison to the previous research and could be used for engineers' preliminary assessments.

### Secondary column axial forces

In this section, results of secondary column axial forces monitored from SAP2000 are examined. The investigation of the effects of forces induced only by post-tensioning on

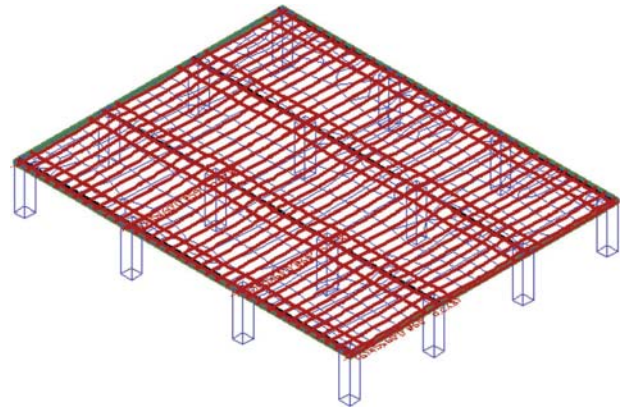


Fig. 14—ADAPT-Builder Floor Pro modeling: office building model with 20 x 25 ft slab panels and 20 x 20 in. columns.

column axial forces showed that the interior columns of the building were consistently in compression, while the exterior columns were in tension. Table 6 shows the secondary column axial forces for each building. For these buildings, the highest force added by the balanced loads was approximately 6 kips on an interior column and 4 kips on an exterior column. This correlates to about 0.3% and 0.2% of the total axial capacity, respectively. This may seem minimal, but these are only two-story buildings. In considering a 50-story building, this increase in force at the foundation level could be as much as approximately 300 kips, which is significant and must be considered during the design process.

This also creates the possibility for differential column shortening between the interior and exterior columns. All concrete columns are expected to shorten during the life of the building; however, the interior columns are subjected to higher magnitudes of force, and therefore may be affected by the secondary forces more than the columns in the exterior of the building. Once again, this effect may be more crucial to consider for buildings with many floor levels. The differential column shortening in the first floor could be approximately 0.5 in. due to the instantaneous elastic effect of post-tensioning for a 75-story building with floor heights of 10 ft, based on the two-story building analysis (Tables 6 to 8) and the following approximation.

$$\delta_1 = \frac{(\Delta P_{avg} + 2\Delta P_{avg} + 3\Delta P_{avg} + \dots + n\Delta P_{avg})L_{col}}{A_g E_c} \quad (10)$$

$$= \frac{\Delta P_{avg} L_{col} \sum_{k=1}^n (k)}{A_g E_c} = \frac{\Delta P_{avg} L_{col} \left( \frac{n(n+1)}{2} \right)}{A_g E_c}$$

**Table 9—Comparison between SAP200 and ADAPT-Builder Floor Pro results**

Bay width, ft	Span length, ft	Column size, in.	Location*	Secondary moment, in.-kip			
				SAP2000 – roof		ADAPT-Builder	
				Exterior frame	Interior frame	Exterior frame	Interior frame
20	25	20 x 20	1	218.7	370.2	77.0	139.6
			2	123.0	218.7	64.7	114.0
			3	3.3	24.8	37.0	111.8
			4	96.2	169.6	61.4	136.9
			5	113.9	201.5	65.3	115.8
		24 x 24	1	223.2	388.4	83.0	158.5
			2	127.5	228.1	66.5	118.2
			3	-2.0	7.1	36.7	98.9
			4	95.5	169.7	65.2	137.0
			5	121.0	215.5	68.3	116.5
		28 x 28	1	223.2	393.6	97.7	162.2
			2	131.6	236.1	70.0	124.2
			3	-5.9	-4.0	32.5	103.0
			4	92.6	165.4	69.2	128.4
			5	127.3	227.9	70.1	119.6
	27	20 x 20	1	244.4	411.9	82.6	146.2
			2	137.3	243.6	75.2	134.2
			3	7.6	34.6	47.0	141.5
			4	104.8	184.7	66.6	161.9
			5	121.6	214.8	80.0	145.3
		24 x 24	1	250.8	435.1	89.9	169.7
			2	142.1	254.0	77.6	139.6
			3	1.0	14.5	46.2	128.8
			4	104.8	186.1	70.7	157.7
			5	129.0	229.6	81.2	147.2
28 x 28	1	251.7	443.1	109.2	180.8		
	2	146.4	262.6	74.5	131.6		
	3	-2.9	2.7	25.3	94.8		
	4	102.7	183.3	65.0	188.9		
	5	135.6	242.5	83.8	150.7		

\*Location 1: exterior end of exterior span (refer to Fig. 7); Location 2: middle of exterior span (refer to Fig. 7); Location 3: interior end of exterior span (refer to Fig. 7); Location 4: interior end of interior span (refer to Fig. 7); and Location 5: middle of interior span (refer to Fig. 7).

$$\delta_{1\_diff} = \delta_{1\_int} - \delta_{1\_ext} \quad (11)$$

where  $\delta_1$  is the secondary column shortening or extension due to post-tensioning at the first-floor level of  $n$ -story building;  $n$  is the total floor level;  $\Delta P_{avg}$  is the average column axial force due to post-tensioning in each slab floor (half the maximum first floor column force in Table 6 was used in this approximation),  $\delta_{1\_diff}$  is the differential column shortening between a corner column and an adjacent interior column at the first floor level; and  $\delta_{1\_int}$  and  $\delta_{1\_ext}$  are the secondary

column axial deformations of adjacent interior and corner columns, respectively, at the first floor level.

Note that in Eq. (10) and (11), the total column deformation was not derived as a summation of the deformations of all floors, but the summation of the column axial forces was only used considering the sequence of construction. More importantly, this approximation does not include creep effects, which may be approximately three times greater than the elastic deformation; thus, further investigation is recommended in this area of research.

**SUMMARY AND CONCLUSIONS**

The primary purpose of this research was to investigate the role of the secondary moment in the design of post-tensioned concrete structures. The design aid charts included in Appendix A can be useful for practicing engineers during the preliminary design of buildings of similar dimensions and loads. These charts can be used as a quick check in the determination of the secondary moment, which can be difficult to calculate at the initial design stage. Furthermore, this research also sought to quantify the effects of post-tensioning on the column axial forces of structures in an effort to investigate the increased loads due to the addition of the secondary moment, as well as the possibility of differential column shortening. While the columns carry the factored gravity loads sufficiently, a significant amount of additional load due to post-tensioning may affect the structural stability of the buildings. This is important to consider because of the added downward force at the locations of the interior columns, which is due to the profile of the tendon. These forces also affect the shortening of the concrete columns and have the potential to cause differential shortening between the interior and exterior (particularly corner) locations. All of these issues are especially important in the design and construction of buildings with many stories.\*

**ACKNOWLEDGMENTS**

The research presented in this paper was funded by the U.S. DOT-RITA (Grant No. DTRT06-G-0016/OTCREOS10.1-21) and the University of Oklahoma, Norman, OK. The authors would like to thank F. Aalami, President of the ADAPT Corporation, for generously donating the ADAPT-Builder Floor Pro program for this research. The authors also would like to acknowledge PTI DC-20: Building Design Committee members R. Ahmed, J. Ales, B. Allred, P. Antis, A. Baxi, M. Cuadra, C. Hayek, J. Hirsch, D. Kline, C. Kopczynski, and M. Vejvoda for their active discussion concerning the design of post-tensioned buildings during committee meetings and conference calls. The views expressed are those of authors and do not necessarily represent those of the sponsors, donor, or discussants.

**REFERENCES**

Aalami, B. O., and Bommer, A., 1999, "Design Fundamentals of Post-Tensioned Concrete Floors," Post-Tensioning Institute, Phoenix, AZ, 184 pp.

ACI Committee 318, 2008, "Building Code Requirements for Structural Concrete (ACI 318-08) and Commentary," American Concrete Institute, Farmington Hills, MI, 473 pp.

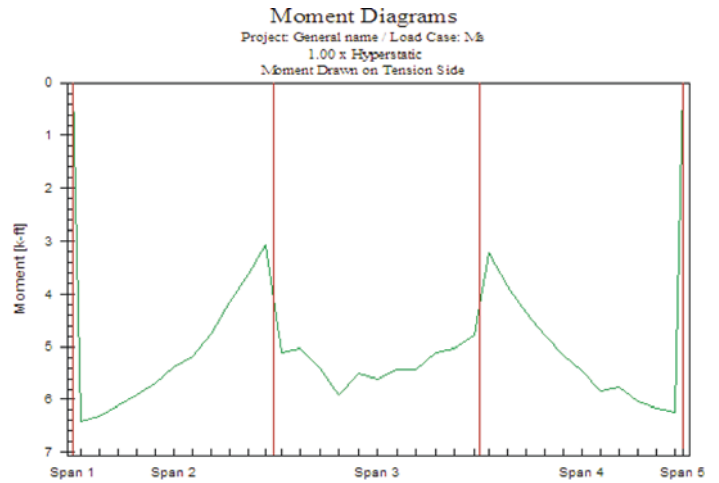


Fig. 15—ADAPT-Builder Floor Pro results: secondary moment diagram of exterior frame for office building model with 20 x 25 ft slab panels and 20 x 20 in. columns.

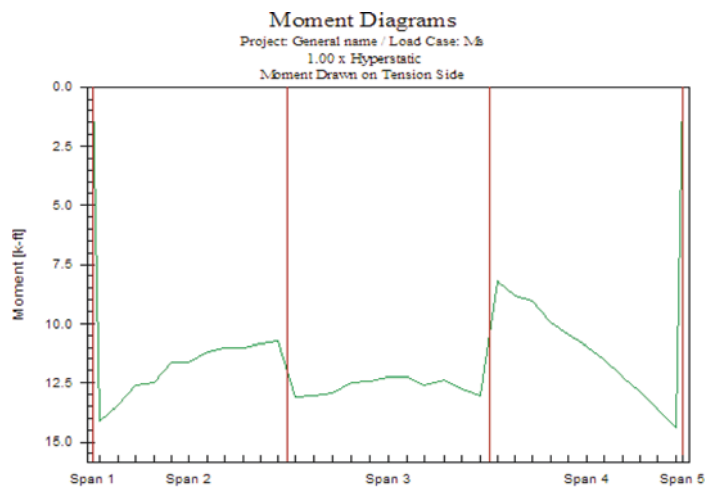


Fig. 16—ADAPT-Builder Floor Pro results: secondary moment diagram of interior frame for office building model with 20 x 25 ft slab panels and 28 x 28 in. columns.

ADAPT, 2010, "ADAPT-Builder Floor Pro 2010," ADAPT Corp., Redwood City, CA.

CSI, 2009, "SAP2000 Tutorial Manual," Computers and Structures Inc., Berkeley, CA, 50 pp.

Foutch, D. A.; Gamble, W. L.; and Sunidja, H., 1990, "Tests of Post-Tensioned Concrete Slab-Edge Column Connections," *ACI Structural Journal*, V. 87, No. 2, Mar.-Apr., pp. 167-179.

Hufnagel, A. C., 2011, "Analytical Studies of Reinforced and Post-Tensioned Concrete Flat-Plate Systems," MS thesis, School of Civil Engineering and Environmental Science, University of Oklahoma, Norman, OK, 222 pp.

Kang, T. H.-K., 2004, "Shake Table Tests and Analytical Studies of Reinforced and Post-Tensioned Concrete Flat Plate Frames," PhD dissertation, Department of Civil & Environmental Engineering, University of California, Los Angeles, Los Angeles, CA, 309 pp.

Kang, T. H.-K., and Wallace, J. W., 2005, "Dynamic Responses of Flat Plate Systems with Shear Reinforcement," *ACI Structural Journal*, V. 102, No. 5, Sept.-Oct., pp. 763-773.

Kang, T. H.-K., and Wallace, J. W., 2008, "Stresses in Unbonded Tendons of Post-Tensioned Flat Plate Systems

under Dynamic Excitation," *PTI Journal*, V. 6, No. 1, Feb., pp. 31-44.

Lin, T. Y., and Burns, N. H., 1981, *Design of Prestressed Concrete Structures*, third edition, Wiley, Hoboken, NJ, 646 pp.

Nilson, A. H.; Darwin, D.; and Dolan, C. W., 2009, *Design of Concrete Structures*, fourteenth edition, McGraw-Hill, New York, 816 pp.

PTI Committee DC-20, 2010, private communication.

PTI Committee DC-20, 2011, "Guide for Design of Post-Tensioned Buildings (PTI DC20.9-11)," Building Design Committee, Post-Tensioning Institute, Farmington Hills, MI, 74 pp.

**Amy Hufnagel** is a Structural Engineer at Walter P Moore, Houston, TX, and is a licensed Engineer-in-Training in Oklahoma. She received her MS and BS from the University of Oklahoma, Norman, OK. She was awarded the 2011 Edward K. Rice Memorial Scholarship from the Post-Tensioning Institute (PTI). Her research interests include analytical and experimental studies of reinforced, prestressed, and post-tensioned concrete structures.

PTI Fellow **Thomas H.-K. Kang** is an Assistant Professor at Seoul National University, Seoul, Korea, and is a licensed Professional Engineer in California. He received his PhD from the University of California, Los Angeles (UCLA), Los Angeles, CA; and his BS from Seoul National University. He is a member of PTI Committee DC-20, Building Design. His research interests include design and rehabilitation of post-tensioned buildings and systems.



Submit contributions to your **JOURNAL**:

**RESEARCH**  
Research involving post-tensioned concrete structures

**CASE STUDIES**  
Applications of post-tensioning illustrating innovation, performance, economics, and sustainability

For more details and submission deadlines, please contact:  
Miroslav Vejvoda, Editor-in-Chief, *PTI JOURNAL*  
E-mail: [miroslav.vejvoda@post-tensioning.org](mailto:miroslav.vejvoda@post-tensioning.org)  
Phone: (248) 848-3184

Paper submittal requirements are outlined in the *PTI JOURNAL* Publication Policy available online at:  
[www.post-tensioning.org/pti\\_journal.php](http://www.post-tensioning.org/pti_journal.php)